Journal of Alloys and Compounds 509 (2011) 3252–3256

Contents lists available at ScienceDirect

Journal of Alloys and Compounds

journal homepage: www.elsevier.com/locate/jallcom

Review

On the general outline of physical properties of amorphous-nanocrystalline Fe–Cr–Mn–N alloy powders prepared by mechanical alloying under nitrogen

R. Amini [a], E. Salahinejad [b,*], E. Askari Bajestani [b], M.J. Hadianfard [b]

[a] Department of Materials Science and Engineering, Shiraz University of Technology, Modarres Blvd., 3619995161, Shiraz, Iran
[b] Department of Materials Science and Engineering, School of Engineering, Shiraz University, Zand Blvd., 7134851154, Shiraz, Iran

ARTICLE INFO

Article history:
Received 19 October 2010
Received in revised form 8 December 2010
Accepted 12 December 2010
Available online 22 December 2010

Keywords:
Metals and alloys
Nanostructured materials
Amorphous materials
Mechanical alloying

ABSTRACT

This paper reviews last findings about physical properties of Fe–Cr–Mn–N powders synthesized by mechanical alloying under nitrogen. Their thermal, magnetic, indentation, and grain growth behaviors and nitrogen distribution in their amorphous-nanocrystalline structure are regarded as a function of milling time. Particularly, the role of nitrogen in the aforementioned phenomena is reviewed in detail.

Contents

1. Introduction

Nickel-free stainless steels are potential substitutes for traditional stainless steels, due to biocompatibility, low cost, good mechanical and corrosion properties [1–6]. To compensate the austenite-stabilizing effect of nickel, the addition of such element(s) as cobalt, copper, carbon, nitrogen, and manganese is required [2,3]. Nitrogen in stainless steels is a strong austenite stabilizer and significantly improves their mechanical properties [7–11] and corrosion resistance [11–13]. In general, nitrogen-containing stainless steels are processed by complex liquid-state methods, especially pressurized electro-slag remelting under high pressures of nitrogen gas [1,2,4]; however, the nitrogen solubility in the liquid phase is limited due to the nitride formation. Because of this, solid-state processes like mechanical alloying (MA) have been regarded as an alternative to synthesize these alloys. Nitrogen alloying through MA can be accomplished by either milling under a nitrogen atmosphere or milling with proper nitride powders.

MA of stainless steels with metallic nitrides under an argon atmosphere has been frequently studied in terms of amorphization [14,15], grain refinement [15], and austenitization behaviors [16,17]. In addition, their microstructural evolutions like phase transformation and grain growth during subsequent heat treatment, consolidation, and mechanical properties have been investigated [18–22]. In the recent years, noticeable researches on MA of stainless steels under a nitrogen atmosphere have been also reported. This paper aims to outline last findings on physical properties of these mechanically alloyed stainless steel powders, consisting of their nitrogen distribution, thermal, magnetic, indentation, and grain growth behaviors.

* Corresponding author. Tel.: +98 917 3879390; fax: +98 711 2307293.
E-mail address: erfan.salahinejad@gmail.com (E. Salahinejad).

0925-8388/$ – see front matter © 2010 Elsevier B.V. All rights reserved.
doi:10.1016/j.jallcom.2010.12.097

2. Structural snapshot

The structure of Fe–Cr–Mn–N alloy powders synthesized by mechanical alloying under nitrogen can be regarded in terms of nitrogen supersaturation, structural refinement, and phase transformation. In order to enter into the main subject, i.e. the physical properties of the Fe–Cr–Mn–N alloy powders, a general view on the structure of this type of materials is briefly presented. During milling under nitrogen gas, molecular nitrogen adheres on virgin surfaces created during MA, dissociates, and consequently penetrates into the powders. Since the amount of structural defects generated by severe plastic deformation during milling is significantly high and since the mismatch strain of nitrogen atoms is reduced in the defects, considerable amounts of nitrogen atoms are infused to the powders, leading to nitrogen supersaturation [23–38].

During MA, the powder particles are subjected to severe plastic deformation, increasing the density of dislocations and forming shear bands containing a high dislocation density. Dislocation cells and subgrains separated by low-angle grain boundaries are formed to decrease the lattice strain. Consequently, the transformation of the low-angle to high-angle grain boundaries takes place by grain rotation, giving nanostructures [39,40]. It has also been realized that the grain refinement in stainless steel powders milled under nitrogen occurs more rapidly and more significantly than in those milled under argon [27]. Diffused nitrogen atoms are segregated at dislocations and grain boundaries, fixing the dislocations and stabilizing the grain boundaries [41]. Afterward, the trickling down of mobile dislocations on the fixed dislocations contributes to the nucleation of new boundaries and severe grain refinement [25].

During MA of stainless steels under nitrogen, austenitization and amorphization transformations have been pointed out [27–31]. The ferrite-to-austenite phase transformation can be explained via the positive role of nitrogen in austenite stabilizing. Nitrogen atoms diffuse into interstitial sites of ferrite crystallites and produce mismatch strains. Austenite has larger interstitial sites than ferrite, implying that nitrogen atoms in austenite create less distortion and volume mismatch. In addition, austenite has smaller interfacial energy compared to ferrite [27]. Apart from the nitrogen effect, the structure refinement to the nanometric scale favors the austenitization transition during MA [33,35]. On the other hand, according to a quantitative amorphous phase analysis based on the Rietveld method [27], by increasing milling time and consequently nitrogen content, the amorphous content increases [27–31]. Amorphization can be explained via high energy given to the powders during milling and the effect of nitrogen on the increase in the atomic size mismatch and heat of mixing of the alloys [27–31]. Typically, Fig. 1 represents a transmission electron microscopy micrograph of Fe–18Cr–8Mn–0.9N alloy powder milled for 48 h under nitrogen. The corresponding selected area diffraction patterns suggest that the dark regions are a combination of the nanocrystalline ferrite and austenite phases, and the bright matrix represents a homogenous hallo pattern attributed to the amorphous structure [42].

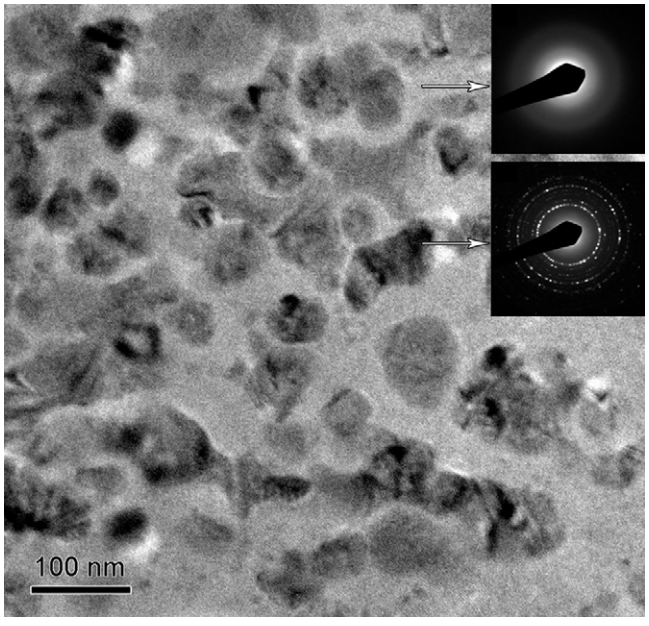

Fig. 1. Transmission electron micrograph of the Fe–18Cr–8Mn–0.9N alloy powder milled for 48 h under nitrogen [42].

3. Thermal behavior

The assessment of the thermal behavior of mechanically alloyed powders is a valuable technique to identify their nature and thermal stability. Typically, Fig. 2 shows differential scanning calorimetry profiles of Fe–18Cr–4Mn–*x*N alloy powders milled for 18–144 h, demonstrating two events during heating. The first exothermic reaction is related to austenite-to-ferrite transformation [27,30]. It is in good agreement with the thermodynamic model proposed by Meng et al. [43] implying that austenite is stable at high temperatures. The second reaction corresponds to the crystallization of the amorphous phase to ferrite and nitrides [27,30].

The amorphous phase developed by MA under nitrogen presents a significant supercooled liquid region, for example 95 K in the Fe–18Cr–4Mn–3.95N alloy [29,30]. These amorphous alloy powders with the wide supercooled liquid regions are capable of being formed into bulk materials with large dimensions, via considerable viscous flow inherent to the supercooled liquid. It has been realized that by increasing nitrogen concentration, the supercooled liquid regions increase [29,30]. According to the Inoue's empirical rules

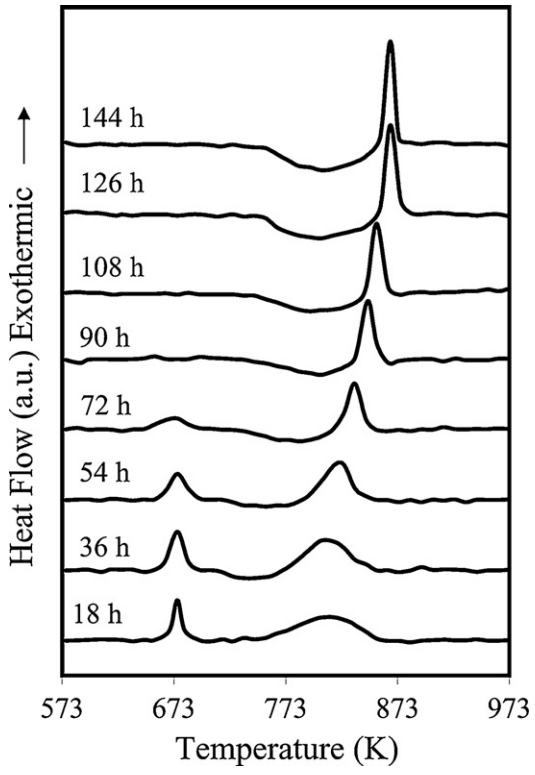

Fig. 2. Differential scanning calorimetry scan of the Fe–18Cr–4Mn–*x*N alloys milled for 18–144 h [30].

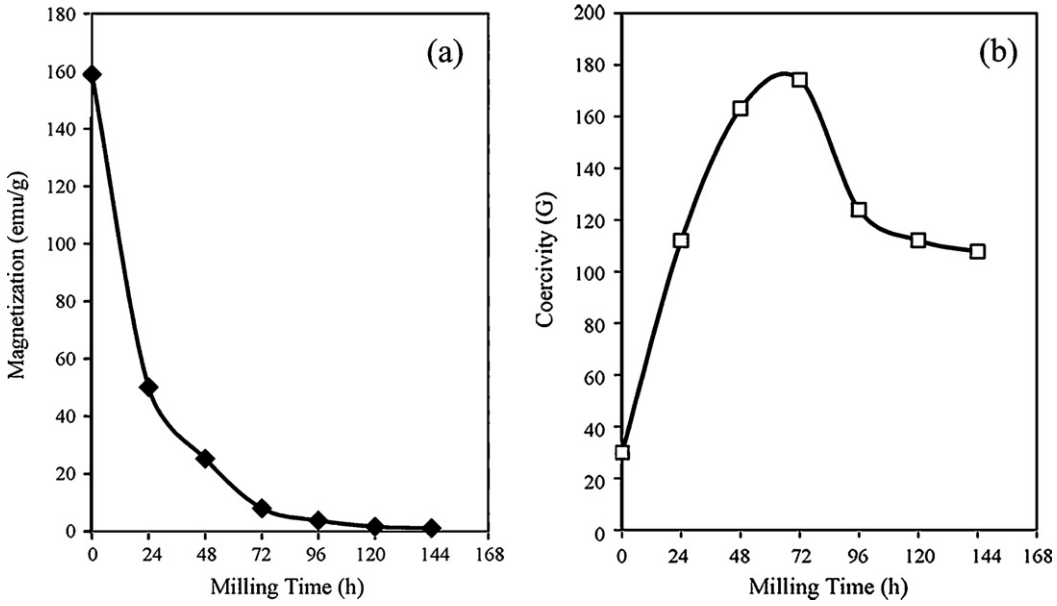

Fig. 3. Variations of the saturation magnetization (a) and coercivity (b) of the Fe–18Cr–12Mn–*x*N alloys vs. milling time [28].

[44,45], the glass-forming ability of amorphous phases depends on (i) the number of the constituent elements, (ii) the atomic size mismatch, and (iii) the heat of mixing among the constituent elements. To have a considerable glass-forming ability, the powder should consist of more than two elements, disturbing the crystal formation by imposing a chemical disorder [29]. This condition is satisfied for both the Fe–Cr–Mn–N and Fe–Cr–Mn alloy systems. A large atomic size mismatch among the elements prevents the formation of a crystalline solid solution. Moreover, a large negative heat of mixing among the elements increases the viscosity of the supercooled liquid [29], suppressing atomic diffusions required for the precipitation of crystals. Since N is far from Fe, Cr, and Mn elements in the periodic table, the addition of nitrogen to Fe–Cr–Mn alloys leads to a considerable increase in the atomic size differences and the negative heats of mixing, increasing the glass-forming ability significantly.

The kinetics of the redistribution of the constituent elements for crystallization is also a critical factor affecting the glass-forming ability. Nitrogen makes the atomic redistribution difficult in stainless steels. Nitrogen atoms by occupying interstitial sites of the atomic polyhedra or clusters increase the dense random packing, thereby increasing the viscosity of the supercooled liquid. Additionally, nitrogen atoms disrupt the short-range order of the amorphous structure, retarding the formation of crystal nuclei. On the other hand, due to the high affinity of these transition metals for nitrogen, nitrogen atoms are surrounded by the metallic atoms, providing the stiff bonds and suppressing the atomic rearrangement required for the precipitation of crystals [29,30].

4. Magnetic properties

In some applications like biomaterials, it is necessary for the candidate material to have a negligible response to electromagnetic fields. Since nickel-free stainless steels are potential materials in biomedical applications, it is of interest to examine their magnetic properties. The saturation magnetization and coercivity of Fe–18Cr–12Mn–*x*N alloys produced by MA under nitrogen have been recently studied. It has been reported that the saturation magnetization of the mechanically alloyed stainless steels is reduced by increasing milling time and nitrogen concentration (Fig. 3a). However, by increasing milling time the coercivity first increases when milling time is less that 96 h and then decreases when it exceeds 96 h (Fig. 3b) [28].

The decrease in the saturation magnetization is discussed from the viewpoints of the nitrogen infusion and the progress of the phase transformations with milling time. By progression of MA, the nitrogen incorporation proceeds; therefore, the nominal percentage of iron having a large net magnetic moment and accordingly the saturation magnetization decrease, on the one hand. In addition, increasing milling time results in the progress of the ferrite-to-austenite transformation and amorphization, reducing the saturation magnetization considerably [28]. The coercivity signifies two different trends at the low and high milling times. The increase in the amount of microstrain and defects, on the one hand, and the decrease in the magnetic ferrite content, crystallite size and saturation magnetization by progression of MA increase the coercivity at the low milling times. Nonetheless, the decrease in the coercivity at the high milling times has been attributed to the extreme grain refinement of ferrite and amorphization from this magnetic phase [28,46,47].

5. Indentation response

The study of the indentation response of amorphous materials is an approach to recognize their hardness and mechanism of plastic deformation on micro and nano-scales. Similar to all amorphous materials, substantial hardness values have been measured for fully amorphous Fe–18Cr–4Mn–*x*N as-milled powders, attributed to the strong bonding between the constituent elements [29]. Interestingly, in contrast to crystalline Fe-based alloys [7–11], the hardness of these amorphous alloys decreases monotonically by increasing nitrogen content [29].

Because of strong interatomic interactions between these transition metals (Fe, Cr, and Mn) and nitrogen, notably the Cr–N pairs [14,27–30,34], some electrons in the metallic bonds are transferred to the metal–nitrogen bonding regions. Since N atoms possess a higher electronegativity than Fe, Cr, and Mn atoms, a strong accumulation of electrons forms towards N atoms. This leads to a depletion of electrons near Fe, Cr, and Mn atoms and consequently the weakening of the metallic bonds. Under these conditions, shear bands can initiate from the weakened intercluster regions, leading to a decrease in the hardness by increasing nitrogen content [29].

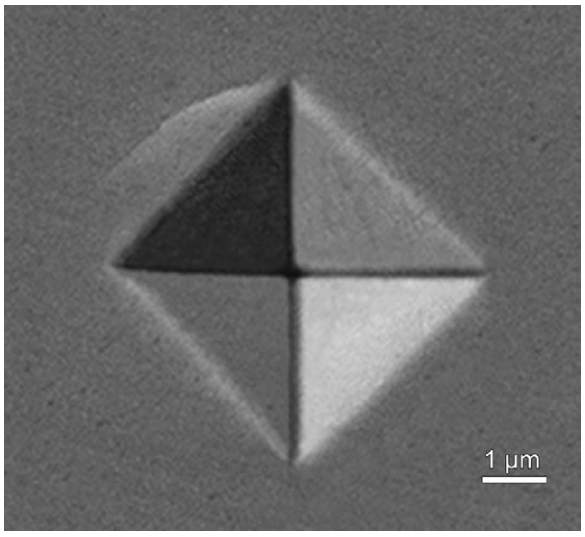

Fig. 4. Scanning electron microscopy micrograph obtained from the upper surface of the indented Fe–18Cr–4Mn–3.62N alloy [29].

The plastic deformation mechanism is determined by observing the morphology of the indented surfaces by scanning electron microscopy (SEM). Fig. 4 represents the SEM image of an indented Fe–18Cr–4Mn–3.62N alloy powder particle. The semicircular shear band markings formed around the indentation impressions imply an inhomogeneous deformation mechanism. The absence of any visible crack demonstrates that the material has an elastic–plastic deformation mode during indentation [29].

Berkovich indentation studies on amorphous materials containing pre-indentation traces have suggested that the material near the traces presents lower hardness and pile-up compared with that far from the trace, due to interactions between the pre-existing and new shear bands [48]. Since the amorphous powder particles prepared by MA have been subjected to severe impacts of the grinding media, they contain numerous shear bands. Accordingly, it can be inferred that the amorphous as-milled materials essentially have higher hardness values, larger pile-ups and more shear bands in the absence of the pre-introduced shear bands induced by milling [29].

6. Grain growth kinetics

Mechanically alloyed high-nitrogen stainless steels represent a considerable thermal stability associated with an inherent resistance to grain growth. Typically, the austenite grain size of mechanically alloyed Fe–Cr–Mn–N alloys before and after a heat treatment is listed in Table 1. It can be seen that the crystallite sizes are still preserved in the nanometeric scale and no significant grain growth occurs.

The kinetics of grain growth is governed by grain boundary mobility. The main factors affecting grain boundary mobility in nanostructures are grain boundaries segregation, solute impurity, porosity, chemical ordering, and secondary phases [32,42,49]. In the high-nitrogen stainless steels synthesized by MA, the retarded grain growth causing the development of nanostructures after annealing and sintering is attributed to the segregation of nitrogen atoms to grain boundaries and the retarded crystallization of the amorphous phase existing in the as-milled powder [42,49–51]. Since the nitrogen solubility in crystalline structures is limited, nitrogen atoms segregate at grain boundaries to decrease strain energy. Typically, it has been found that only about 4% of total incorporated nitrogen is distributed among crystal interstitial sites of the Fe–18Cr–8Mn–2.5N alloy synthesized by MA [52]. Thus, the considerable amount of nitrogen is distributed among other sites of the structure, including grain boundaries [52]. The accumulation of considerable nitrogen contents at grain boundaries retards grain growth. Additionally, the stability of the amorphous phase created during MA is significant [27–30,42,49]. That is, the crystallization of this phase is expected to be a slow transformation, affecting the resultant grain size.

Table 1
Austenite grain size of mechanically alloyed stainless steels: as-milled (d_0), after a heat treatment (d), heat treatment temperature (T), and heat treatment time (t).

Alloy composition (wt.%)	d_0 (nm)	d (nm)	T (°C)	t (h)	Reference
Fe–18Cr–11Mn–1.7N	4.6	35	1200	2	[32]
Fe–18Cr–8Mn–0.9N	11	90	1100	20	[42,49,51]
Fe–18Cr–8Mn–1.3N	8.1	88	1100	20	[51]
Fe–18Cr–8Mn–1.8N	6.2	87	1100	20	[51]
Fe–18Cr–8Mn–2.1N	5.1	85	1100	20	[51]

It would be worth noting that in Refs. [32–34,42,49–51], the stainless steel samples have been encapsulated in quartz tubes to prevent oxidation in annealing and sintering examinations. The application of the encapsulation technique results in the insulation of the samples in a small closed volume, thereby preserving nitrogen and supporting the stability [42,49–51]. Moreover, the presence of elements like Cr, Mn, Ta, and Nh having a high affinity for nitrogen in stainless steels prevents nitrogen from escaping at high temperatures [17].

7. Nitrogen partitioning

The nitrogen infusion into the materials can be accompanied with (i) the precipitation of nitrides, (ii) the dissolution into interstitial sites of crystallites, (iii) the segregation at defects like grain boundaries and dislocations, and (iv) the distribution among interstitial sites of the amorphous phase. Recently, a method has been introduced to estimate nitrogen partitioning in the structure of nanocrystalline-amorphous alloys, based on X-ray diffraction, thermogravimetry, and differential scanning calorimetery [53]. The contribution of crystal interstitial sites (N_{int}) is estimated by the X-ray diffraction method from changes in interplanar spacing [52,53], and the amounts of nitrogen in defects (N_{def}) and amorphous phase (N_A) are determined by thermogravimetry and differential scanning calorimetery [53]. Table 2 tabulates the related results for Fe–18Cr–8Mn powder synthesized by MA under nitrogen. The first increase in N_{int} is because of the domination of the ferrite-to-austenite phase transformation providing larger crystal interstitial sites. Afterwards, nitrogen saturation in the crystal interstitial sites is resulted and also the amorphization transition prevails. It is also noticeable that by progression of milling, the contribution of the defects and amorphous phase to the nitrogen incorpora-

Table 2
Structure and nitrogen contents (wt.%) in Fe–18Cr–8Mn powders milled under nitrogen [53].

Milling time (h)	α-Phase percentage	γ-Phase percentage	Amorphous percentage	N_{int}	N_{def}	N_A
24	51.7	19.3	29.0	0.26	0.13	0.30
72	17.7	38.6	43.7	0.34	0.21	0.78
120	5.3	27.3	67.4	0.23	0.45	1.45
168	0	0	100	0	0	2.95

tion increases. It is due to the fact that the defect density and the amorphous phase amount increase by increasing the milling time; nitrogen atoms prefer to go to these sites to decrease the strain energy. The results indicate that the amorphous phase plays a crucial role in the nitrogen supersaturation.

8. Concluding remarks

Aspects of physical properties of stainless steel powders produced by MA under a nitrogen atmosphere were outlined. MA under these conditions introduces nitrogen into the matrix, through a solid–gas reaction. Ferrite-to-austenite phase transformation and amorphization occur during MA, leading to the development of nanostructured-amorphous powders. The amorphous phase exhibits a considerable glass-forming ability that increases by increasing nitrogen concentration. By increasing milling time, the saturation magnetization decreases; nonetheless, the coercivity first increases and then decreases. The microhardness of fully amorphous Fe–Cr–Mn–N alloys synthesized by MA decreases by increasing nitrogen content. The amorphous material presents an elastic–plastic deformation mode during indentation experiments. Mechanically alloyed high-nitrogen stainless steels depict a considerable resistance to grain growth during annealing and sintering. In addition the amorphous phase plays a crucial role in the nitrogen supersaturation.

References

[1] N. Nakada, N. Hirakawa, T. Tsuchiyama, S. Takaki, Scripta Mater. 57 (2007) 153–156.
[2] G. Balachandran, M.L. Bhatia, N.B. Ballal, P.K. Rao, ISIJ Int. 41 (2001) 1018–1027.
[3] K. Alvarez, K. Sato, S.K. Hyun, H. Nakajima, Mater. Sci. Eng. C 28 (2008) 44–50.
[4] M. Sumita, T. Hanawa, S.H. Teoh, Mater. Sci. Eng. C 24 (2004) 753–760.
[5] J. Menzel, W. Kirschner, G. Stein, ISIJ Int. 36 (1996) 893–900.
[6] P.J. Uggowitzer, R. Magdowski, M.O. Speidel, ISIJ Int. 36 (1996) 901–908.
[7] J. Rawers, M. Grujicic, Mater. Sci. Eng. A 207 (1996) 188–194.
[8] D.W. Kim, W.S. Ryu, J.H. Hong, S.K. Choi, J. Nucl. Mater. 254 (1998) 226–233.
[9] J.B. Vogt, J. Mater. Process. Technol. 117 (2001) 364–369.
[10] J. Freudenberger, A. Gaganov, A.L. Hickman, H. Jones, Cryogenics 43 (2003) 133–136.
[11] J.W. Simmons, Mater. Sci. Eng. A 207 (1996) 159–169.
[12] I. Olefjord, L. Wegrelius, Corros. Sci. 38 (1996) 1203–1220.
[13] H. Baba, T. Kodama, Y. Katada, Corros. Sci. 44 (2002) 2393–2407.
[14] H. Miura, K. Omuro, H. Ogawa, ISIJ Int. 36 (1996) 951–957.
[15] H. Ogawa, K. Omuro, H. Miura, Mater. Sci. Forum 318 (1999) 687–694.
[16] H. Miura, H. Ogawa, K. Omuro, Mater. Sci. Forum 318 (1999) 707–714.
[17] H. Miura, H. Ogawa, Mater. Trans. 42 (2001) 2368–2373.
[18] R. Murakami, Y. Aoyama, N. Tsuchida, Y. Harada, K. Fukaura, Mater. Sci. Forum 561–565 (2007) 37–40.
[19] T. Tsuchiyama, H. Uchida, K. Kataoka, S. Takaki, ISIJ Int. 42 (2002) 1438–1443.
[20] K. Kataoka, T. Tsuchiyama, H. Goto, S. Takaki, Trans. Indian Inst. Met. 56 (2003) 527–531.
[21] H. Uchida, K. Kataoka, T. Tsuchiyama, H. Goto, S. Takaki, J. Jpn. Soc. Powder Metall. 48 (2001) 980–985.
[22] L. Jing, L. Guang-qiang, P. Bing, Z. Xin, Proc. Sino-Swedish Struct. Mater. Symp. (2007) 310–315.
[23] C.J. Rawers, R.C. Doan, Metall. Mater. Trans. A 25 (1994) 381–388.
[24] C.J. Rawers, D. Maurice, Acta Mater. 43 (1995) 4101–4107.
[25] C.J. Rawers, D. Govier, R. Doan, Mater. Sci. Eng. A 22 (1996) 162–167.
[26] J. Rawers, D. Govier, D. Cook, ISIJ Int. 36 (1996) 958–961.
[27] R. Amini, M.J. Hadianfard, E. Salahinejad, M. Marasi, T. Sritharan, J. Mater. Sci. 44 (2009) 136–148.
[28] R. Amini, H. Shokrollahi, E. Salahinejad, M.J. Hadianfard, M. Marasi, T. Sritharan, J. Alloys Compd. 480 (2009) 617–624.
[29] E. Salahinejad, R. Amini, M. Marasi, T. Sritharan, M.J. Hadianfard, Mater. Chem. Phys. 118 (2009) 71–75.
[30] R. Amini, E. Salahinejad, M.J. Hadianfard, M. Marasi, T. Sritharan, Mater. Sci. Eng. A 527 (2010) 1135–1142.
[31] E. Salahinejad, R. Amini, E. Askari Bajestani, M.J. Hadianfard, J. Alloys Compd. 497 (2010) 369–372.
[32] M.M. Cisneros, H.F. Lopez, H. Mancha, D. Vazquez, E. Valdes, G. Mendoza, M. Mendez, Metall. Mater. Trans. A 33 (2002) 2139–2144.
[33] M.M. Cisneros, H.F. Lopez, H. Mancha, E. Rincon, D. Vazquez, M.J. Perez, S.D.D.L. Torre, Metall. Mater. Trans. A 36 (2005) 1309–1316.
[34] M. Mendez, H. Mancha, M.M. Cisneros, G. Mendoza, J.I. Escalante, H.F. Lopez, Metall. Mater. Trans. A 33 (2002) 3273–3278.
[35] T. Haghir, M.H. Abbasi, M.A. Golozar, M. Panjepour, Mater. Sci. Eng. A 507 (2009) 144–148.
[36] D. Cui, X. Qu, P. Guo, K. Li, Powder Metall. Technol. 26 (2008) 265–268.
[37] L. Guan, X. Qu, C. Jia, S. Wang, J. Univ. Sci. Technol. Beijing 27 (2005) 692–694.
[38] T. Fukutsuka, T. Anzai, M. Kaneda, Y. Matsuo, Y. Sugie, K. Fukaura, J. Soc. Mater. Sci. Jpn. 53 (2004) 1175–1179.
[39] C. Suryanarayana, Prog. Mater. Sci. 46 (2001) 1–184.
[40] C. Suryanarayana, E. Ivanov, V.V. Boldyrev, Mater. Sci. Eng. A 304–306 (2001) 151–158.
[41] Y. Ogino, S. Murayama, T. Yamasaki, J. Less-Common Met. 168 (1991) 221–235.
[42] E. Salahinejad, R. Amini, M. Marasi, M.J. Hadianfard, Mater. Des. 31 (2010) 527–532.
[43] Q. Meng, N. Zhou, Y. Rong, S. Chen, T.Y. Hsu, X. Zuyao, Acta Mater. 50 (2002) 4563–4570.
[44] A. Inoue, T. Zhang, T. Masumoto, J. Non-Cryst. Solids 156–158 (1993) 473–480.
[45] A. Inoue, Mater. Trans. Jpn. Inst. Met. 36 (1995) 866–875.
[46] M.E. McHenry, M.A. Willard, Prog. Mater. Sci. 44 (1999) 291–433.
[47] E. Kita, N. Tsukuhara, H. Sato, K. Ota, H. Yangaihara, H. Tanimoto, N. Ikeda, Appl. Phys. Lett. 88 (2006) 152501-1–152501-3.
[48] C. Tang, Y. Li, K. Zeng, Mater. Lett. 59 (2005) 3325–3329.
[49] E. Salahinejad, R. Amini, M. Marasi, M.J. Hadianfard, Mater. Des. 31 (2010) 2259–2263.
[50] E. Salahinejad, R. Amini, M.J. Hadianfard, Mater. Des. 31 (2010) 2241–2244.
[51] E. Salahinejad, R. Amini, M.J. Hadianfard, Mater. Sci. Eng. A 527 (2010) 5522–5527.
[52] E. Salahinejad, R. Amini, M. Ghaffari, M.J. Hadianfard, J. Alloys Compd. 505 (2010) 584–587.
[53] R. Amini, E. Salahinejad, M.J. Hadianfard, E. Askari Bajestani, M. Sharifzadeh, J. Alloys Compd. (2010) 194, doi:10.1016/j.jallcom.2010.10.